Published in final edited form as:
Neuron. 2011 January 27; 69(2): 258–272. doi:10.1016/j.neuron.2011.01.001.

The Molecular and Cellular Basis of Bitter Taste in *Drosophila*

Linnea A. Weiss[1], **Anupama Dahanukar**[1,2], **Jae Young Kwon**[1,3], **Diya Banerjee**[1], and **John R. Carlson**[1,*]

[1]Department of Molecular, Cellular and Developmental Biology, Yale University, New Haven, CT 06520-8103, USA

[2]Department of Entomology, University of California, Riverside, CA 92521, USA

[3]Department of Biological Sciences, Sungkyunkwan University, Suwon 440-746, Republic of Korea

Summary

The extent of diversity among bitter-sensing neurons is a fundamental issue in the field of taste. Data are limited and conflicting as to whether bitter neurons are broadly tuned and uniform, resulting in indiscriminate avoidance of bitter stimuli, or diverse, allowing a more discerning evaluation of food sources. We provide a systematic analysis of how bitter taste is encoded by the major taste organ of the *Drosophila* head, the labellum. Each of 16 bitter compounds is tested physiologically against all 31 bitter neurons, revealing responses that are diverse in magnitude and dynamics. Four functional classes of bitter neurons are defined. Four corresponding classes are defined through expression analysis of all 68 Gr taste receptors. A receptor-to-neuron-to-tastant map is constructed. Misexpression of one receptor confers bitter responses as predicted by the map. These results reveal a degree of complexity that greatly expands the capacity of the system to encode bitter taste.

Introduction

Understanding of a sensory system depends critically on the definition of the neuronal classes it comprises. Our understanding of human color vision, for example, rests on the classic definition of three classes of photoreceptor cells, the determination of their spectral sensitivities, and the identification of the opsins that underlie the sensitivity of each (Nathans, 1989).

Animals rely on taste systems to detect toxins, which are often perceived as bitter. When taste organs make contact with a potential food source, the presence of bitter compounds is signaled by taste cells to the CNS. This input informs a decision that is critical to the animal's survival: acceptance or rejection.

A central problem in the field of taste has been to define the bitter-sensitive neurons, their response spectra, and the receptors that impart their molecular specificity. Are bitter-sensitive cells tuned broadly and uniformly, leading to indiscriminate avoidance of potentially toxic substances, or are they diverse and more selectively tuned, providing the

*Correspondence: john.carlson@yale.edu.

capacity for a more informative assessment of complex food sources? A comprehensive definition of the molecular and cellular basis of bitter taste across an entire taste organ is needed to allow basic principles of bitter coding to emerge. Such an analysis has not been performed in invertebrates and is difficult to perform in mammals due to the complexity of mammalian taste organs.

The labellum of *Drosophila* offers several advantages in the study of bitter taste. The organ is numerically simple. Each half of the labellum contains 31 prominent sensilla called taste hairs, most containing one bitter-sensitive neuron. The responses of all of these bitter-sensitive neurons can be measured *in vivo* by physiological recording. A large family of taste receptor genes, the *Gr* genes, has been defined. Behavioral responses to bitter tastants can be measured and integrated with cellular and molecular analyses.

The taste hairs of the labellum are arranged in a stereotyped pattern, with minor variation among flies. The hairs have been classified into three groups (Shanbhag et al., 2001) and named according to their morphology and position (Hiroi et al., 2002): L (long), I (intermediate) and S (short) (Figure 1A), with each individual sensillum of a class identified by a subscript, *i.e.* L_1. Most hairs contain four taste neurons: one sensitive to sugars, one to low concentrations of salt, one to bitter compounds and high concentrations of salt, and one to water or low osmolarity; I-type hairs contain just two taste neurons, one that responds to sugars and low concentrations of salt, and another that responds to bitter compounds and high concentrations of salt (Dethier, 1976; Falk et al., 1976; Fujishiro et al., 1984; Hiroi et al., 2004; Nayak and Singh, 1983; Rodrigues and Siddiqi, 1978).

The *Gr* family includes 60 members that are predicted to encode 68 seven-transmembrane receptors through alternative splicing (Clyne et al., 2000; Dunipace et al., 2001; Robertson et al., 2003; Scott et al., 2001). Genetic analysis has revealed that *Gr5a* and two closely related genes, all members of a clade of eight *Gr* genes, are required for responses to sugars (Dahanukar et al., 2007; Jiao et al., 2008; Slone et al., 2007). *Gr32a*, *Gr33a*, *Gr66a*, and *Gr93a* are required for responses to caffeine and/or certain other bitter compounds (Lee et al., 2010; Lee et al., 2009; Moon et al., 2006; Moon et al., 2009). Analysis of *Gr-GAL4* drivers has shown that *Gr5a* is expressed in sugar-sensitive neurons in each sensillum, while *Gr66a* is expressed in a distinct population of ~20 neurons that responds to a number of bitter compounds and that mediates aversion (Chyb et al., 2003; Marella et al., 2006; Thorne et al., 2004; Wang et al., 2004). Two *Gr5a*-related genes map to *Gr5a*-expressing neurons, while a number of other *Gr* genes appear to be expressed in subsets of *Gr66a*-expressing neurons (Dahanukar et al., 2007; Lee et al., 2009; Moon et al., 2009; Thorne and Amrein, 2008; Thorne et al., 2004; Wang et al., 2004). The sensilla associated with these subsets have not been identified in most cases, however, and expression of the great majority of *Gr* genes has not been examined.

Historically, a critical question in the field has been whether all taste sensilla are functionally equivalent (Hiroi et al., 2002; Marella et al., 2006; Thorne et al., 2004; Wang et al., 2004). Previous physiological analysis of the labellum revealed that three sensilla, L_7, L_8, and L_9 (Figure 1A), were similar in their responses to all of 50 tested compounds, mostly sugars (Dahanukar et al., 2007). A study of 21 sensilla and four sugars showed that all sensilla responded to all tested sugars, with some quantitative differences among sensilla of different morphology (Hiroi et al., 2002). A survey of a few bitter compounds revealed that none of the longer sensilla on the labellum responded, while all of the shorter hairs that were tested gave indistinguishable responses (Hiroi et al., 2004). An imaging study found that different subpopulations of bitter cells responded to most bitter compounds tested; striking differences in response profiles were not observed (Marella et al., 2006).

Based on these studies, it has been suggested that bitter-sensitive neurons of the labellum may generally recognize the same bitter compounds (Cobb et al., 2009; Marella et al., 2006). A similar model emphasizing functional homogeneity is often cited in mammals, in which multiple bitter receptors are coexpressed and taste receptor cells respond to a broad range of bitter compounds (Adler et al., 2000; Mueller et al., 2005; Yarmolinsky et al., 2009). However, a systematic analysis of the responses of the labellar taste sensilla to bitter compounds, such as those carried out with *Drosophila* olfactory sensilla and odorants (de Bruyne et al., 2001), has not been performed. Due to the limited scope of the extant studies, the basic principles of functional organization that underlie bitter coding in the fly remain unclear.

Here we investigate basic principles of bitter coding through a systematic behavioral, physiological and molecular analysis. We first measure behavioral responses to a panel of diverse bitter compounds and find that the compounds vary greatly in the degree of aversion they elicit. We then test the physiological responses of all 31 labellar taste hairs to 16 diverse bitter tastants. The responses of different sensilla show extensive diversity, both in magnitude and in response dynamics. We define four functional classes of bitter neurons, and the results provide a functional map of the organ. We then examine the expression of all 68 members of the Gr family of taste receptors. Based on receptor expression, the bitter neurons fall into four classes that coincide closely with the four classes based on physiological responses. The results provide a receptor-to-neuron-to-tastant map of the organ. Misexpression of a receptor confers bitter responses that agree with predictions of the map. Together, the results reveal a degree of complexity that greatly expands the capacity of the system to encode bitter taste; it allows for combinatorial coding and may enable discrimination or adaptive responses to selected bitter stimuli.

Results

Bitter compounds elicit differing degrees of aversive behavior

We selected 14 compounds that have previously been described as bitter by virtue of their behavioral effects on various insect species (Koul, 2005; Schoonhoven et al., 2005). The 14 selected tastants include naturally occurring alkaloids, terpenoids, and phenolic compounds, as well as three synthetic compounds. Many of these compounds are toxic, and many are perceived as bitter by humans. Some have been tested in *Drosophila* previously (Hiroi et al., 2004; Lee et al., 2010; Marella et al., 2006; Meunier et al., 2003; Thorne et al., 2004; Wang et al., 2004).

We used a modification of a two-choice behavioral paradigm (Tanimura et al., 1982) in which a population of flies is allowed to feed on a microtiter plate containing alternating wells of 1 mM sucrose alone and 5 mM sucrose mixed with a bitter tastant (Figure 2A). Each of the two solutions contains either red or blue dye, and upon conclusion of the experiment a preference index (P.I.) is calculated. The P.I. is based on the number of flies with red, blue and purple abdomens, indicating ingestion of the solution with red dye, the solution with blue dye, or both solutions, respectively [P.I. = $(N_{blue} + 0.5N_{purple})/(N_{red} + N_{purple} + N_{blue})$].

In our experiments, a P.I. of 1.0 indicates a complete preference for the 5 mM sucrose solution; a P.I. of 0 indicates a complete preference for the 1 mM sucrose solution. We found that in control experiments, flies given a choice between 1 mM sucrose and 5 mM sucrose alone, with no added bitter compounds, showed a P.I. of 0.71, indicating a preference for the 5 mM concentration.

We tested a range of concentrations of the 14 tastants. Low concentrations of each tastant had little or no effect on the strong preference for 5 mM sucrose (Figures 2B and S1). However, with addition of increasing concentrations of each bitter tastant to the 5 mM solution, flies increasingly avoided the 5 mM sucrose-bitter mixture. For all compounds, we identified a concentration at which there was a near complete avoidance of the bitter compound, *i.e.* the P.I. approached 0. For some bitter tastants (*e.g.* azadirachtin and umbelliferone), testing was limited by the low solubility of the tastant, but near-maximal avoidance was observed at the highest concentrations available.

Some bitter compounds were more aversive than others (Figures 2B and 2C). To quantify the sensitivity of the fly to each compound we calculated the concentration of bitter tastant that is required to render 5 mM sucrose equally attractive, or "isoattractive", to 1 mM sucrose. We defined the isoattractive concentration as the concentration at which the P.I. is 0.36, which is the arithmetic mean of the control P.I. (0.71) and the minimal P.I. (0). Thus the isoattractive concentration for denatonium, illustrated in Figure 2B, lies between $10^{-4.5}$ M and 10^{-5} M.

Among our panel of tastants, denatonium elicits the strongest avoidance (Figure 2C). Interestingly, denatonium has also been identified as the tastant that is perceived as most bitter by humans in psychophysical studies (Hansen et al., 1993; Keast et al., 2003). The isoattractive concentrations of our bitter panel ranged over more than two orders of magnitude, with the weakest avoidance elicited by escin (Figure 2C).

These results confirmed that all members of the tastant panel are aversive or "bitter" to *Drosophila* (Figure S1). The results also identified a concentration range over which each bitter compound is behaviorally active in this paradigm. Together these results established a foundation for a detailed physiological analysis of the cellular basis of bitter coding.

Sensilla are diverse in their responses to bitter compounds

As a first step towards understanding the coding of bitter stimuli, we systematically examined the electrophysiological responses (Hodgson et al., 1955) elicited by all 14 bitter substances from all 31 labellar taste sensilla (Figure 1A). These tastants were tested at 1 mM or 10 mM, or 1% in one case, concentrations at which they were active in our behavioral paradigm. We also tested two additional compounds, aristolochic acid and gossypol, described as bitter in other insect species, yielding a total of 16×31=496 sensillum-tastant combinations, each tested n≥10 times.

All 16 compounds elicited action potentials from at least some sensilla. The action potentials were of a large amplitude characteristic of the bitter neuron (Figure 1B). In a few cases we observed a small number of additional action potentials of smaller amplitude, presumably generated by the water neuron, particularly in the initial period of the recording (*e.g.* see "ARI" trace in Figure 1B). Three of the 31 sensilla, S_3, S_5 and S_9, generated a second, high-frequency and low-amplitude spike train of unknown source that appeared to be independent of stimulus identity and concentration (Figure 1C). However, in all cases the large-amplitude action potentials of the bitter neuron could easily be distinguished and are the basis of the analysis that follows.

We found that individual tastants elicit responses from subsets of sensilla, and that individual sensilla are activated by subsets of tastants (Figure 3, Tables S1 and S2). Different sensilla responded to different subsets of stimuli. For example, I_9 and I_{10} responded strongly to theophylline but not denatonium, whereas I_4 and I_5 responded strongly to denatonium but not theophylline (Figure 1D). Inspection of the response matrix

(Figure 3) reveals extensive heterogeneity among the labellar sensilla, and by extension, among the bitter neurons that they contain.

A functional map of labellar taste sensilla

The long (L) sensilla exhibited little or no physiological response to our panel of tastants, in agreement with a previous report (Hiroi et al., 2004). Two of the short sensilla, S_4 and S_8, also did not respond to any bitter tastants. All other S type sensilla were broadly tuned, responding to 9–15 of the 16 compounds with a spike frequency of >10 spikes/s (Figure 3, Tables S1 and S2). I type sensilla were more narrowly tuned with respect to our panel of tastants, responding to 3–7 compounds. The strongest response was elicited by 10 mM caffeine in the S_5 sensillum (60.8 ± 3.3 spikes/s; n = 34).

A hierarchical clustering analysis identified five functional classes of labellar sensilla: two classes of broadly tuned sensilla (S-a and S-b), two classes of narrowly tuned sensilla (I-a and I-b), and a fifth class that did not display excitatory responses to any of our panel of tastants (L, S-c) (Figures 4A and 4B). The two classes of S sensilla are both broadly tuned, but the S-b sensilla exhibit greater mean responses to most tastants (Figure 4B). Notably, this class comprises the three sensilla that uniquely exhibited a second high-frequency action potential (Figure 1C). The more narrowly tuned I-a and I-b sensilla respond to complementary subsets of tastants.

Maps of the distribution of the sensilla of each class are shown in Figure 4C. The most broadly tuned sensilla (S-a and S-b classes) are located in the medial region of the labellum, while the narrowly tuned sensilla (I-a and I-b classes) are in lateral regions. The three classes of S sensilla are intermingled in the row of medial sensilla, while the I-a and I-b sensilla are restricted to the anterior and posterior portions of the labellum, respectively.

We note with interest that among the five bitter compounds that elicited responses >10 spikes/s from the I-a sensilla, three elicited the most aversive behavioral responses (denatonium, sparteine sulfate and lobeline), and one elicited the fifth most aversive response (berberine) (Figure 2C). The median isoattractive concentration for these five tastants was <0.1 mM; the median concentration for all the others was ~1 mM. Although gustatory input from other organs such as the legs is likely to influence this behavior, these results suggest the possibility that different classes of bitter-sensing neurons make different contributions to the behavior of the fly.

Temporal coding of bitter stimuli

Some tastants elicited delayed responses. Four compounds, coumarin, saponin, escin, and gossypol, exhibited delays of >100 ms in discharge (Figure 5A). We quantified these temporal dynamics by measuring the interval between the time at which electrical contact was registered (the contact artifact) and the onset of spike discharge. Different tastants elicited responses with delays of different lengths (Figure 5B). S-a and S-b sensilla showed comparable temporal dynamics for a given tastant. Differences among compounds in spike latency are not restricted to the labellum, but have also been noted in leg sensilla (Meunier et al., 2003).

Other compounds elicited shorter delays in spike onset that differed among sensilla (Figures 5C and 5D). The length of the delay did not show a simple correlation with the magnitude of the response: *e.g.*, I-a and S-a sensilla yielded similar response magnitudes to berberine (28±3 and 27±2 spikes/s, respectively; n = 24–47 sensilla of each individual type, with means for each type averaged across each class), but the delays in response differed by a factor of two (43±2 and 81±6 ms, respectively, n = 12–40). Taken together, these results suggest that such differences in spike onset may represent a salient feature of taste coding.

We note that erratic or "bursting" responses in S-b sensilla are occasionally observed in response to gossypol and strychnine (Figure 5E) as well as berberine, lobeline, sucrose octaacetate, and aristolochic acid. Of the S_5 sensilla that responded to berberine, 63% of traces exhibited a bursting pattern (n = 19). Similar bursts of action potentials were reported for tarsal gustatory sensilla tested with high concentrations of bitter tastants (Meunier et al., 2003); we do not know whether such bursting responses contribute to taste coding.

Coding of bitter intensity

The intensity of bitter substances is a critical factor in evaluating the palatability of a food source. We examined the coding of bitter intensity, with a special interest in the sensitivity and dynamic range of neuronal responses, by systematically testing the responses of representative labellar sensilla to caffeine, denatonium and lobeline, over a wide range of concentrations (Figure S2). All tested sensilla exhibited dose-dependent responses to each compound. In the case of most tastant-sensillum combinations the response threshold lay between 0.1 mM and 1 mM concentrations. While the limited solubility of some tastants precluded a more extensive analysis, the dynamic ranges extended over at least an order of magnitude in most cases. Sugar stimuli at comparable concentrations evoke little if any response from labellar sensilla (Dahanukar et al., 2007; Hiroi et al., 2002), illustrating the sensitivity of bitter responses.

A receptor-to-neuron map reveals distinct classes of bitter neurons

Having analyzed first the behavior driven by bitter compounds and then the cellular basis of bitter response, we next examined its molecular basis. The expression of most *Gr* genes has not been examined, and few have been mapped to individual sensilla (Dahanukar et al., 2007; Hiroi et al., 2002; Koganezawa et al., 2010). *In situ* hybridizations with *Gr* genes have been unsuccessful in most cases (Clyne et al., 2000; Dahanukar et al., 2007; Dunipace et al., 2001; Moon et al., 2009; Scott et al., 2001), perhaps due to low levels of *Gr* expression. However, there has been greater success in analyzing *Gr* expression patterns using the *GAL4/UAS* system to drive reporter gene expression (Brand and Perrimon, 1993; Chyb et al., 2003; Dunipace et al., 2001; Moon et al., 2009; Scott et al., 2001; Thorne and Amrein, 2008).

We have analyzed the expression patterns of all 68 Gr family members using *Gr-GAL4* lines. We generated flies with *Gr-GAL4* transgenes for 59 members of the gustatory receptor family and acquired previously published lines for 8 receptors (Dunipace et al., 2001; Scott et al., 2001; Table S3). One line, *Gr23a-GAL4*, represents two alternatively spliced receptors that share a common 5' region, Gr23a.a and Gr23a.b. For most receptors, 2–6 independent *Gr-GAL4* lines were examined (Table S3).

We found expression in labellar sensilla for 38 *Gr-GAL4* drivers (Figure 6). Some drivers show expression in all labellar sensilla; most show expression in subsets of sensilla. The vast majority of the drivers are expressed in a single neuron of the sensilla in which they are expressed. To identify the neuron we carried out a series of double-label experiments.

Gr5a, a sugar receptor, is expressed in the sugar-sensitive neuron of all labellar sensilla, while Gr66a, a receptor required for caffeine perception, is expressed in all bitter neurons (Thorne et al., 2004; Wang et al., 2004). To mark bitter-sensitive neurons we used a direct fusion of RFP to the *Gr66a* promoter (*Gr66a-RFP*), a construct whose expression pattern matches that of the *Gr66a-GAL4* driver (Dahanukar et al., 2007). The RFP reporter is observed in each of the S and I sensilla, with the exceptions of S_4 and S_8.

Five of the 38 drivers showed no coexpression with *Gr66a-RFP* (Figure S3, upper panel). These five receptors, which include Gr5a, are all known or predicted sugar receptors

(Dahanukar et al., 2007; Jiao et al., 2008; Slone et al., 2007). The remaining 33 labellar *Gr-GAL4* drivers labeled subsets of *Gr66a*-expressing neurons, or all *Gr66a*-expressing neurons (Figure S3, lower panel), and thus may function in bitter taste perception. Our data are consistent with reports that *Gr33a* and *Gr93a*, in addition to *Gr66a*, contribute to the perception of caffeine and other bitter tastants (Lee et al., 2009; Moon et al., 2006; Moon et al., 2009). None of the 33 "bitter" *Gr-GAL4* drivers, with two exceptions (Table S3), was expressed in L, S_4 or S_8 sensilla, consistent with the lack of bitter physiological responses in these sensilla.

Some individual drivers are expressed broadly, *e.g.Gr33a-GAL4* is expressed in all bitter-sensing neurons, whereas others are expressed only in a few, *e.g.Gr22f-GAL4* is expressed only in S_3, S_5 and S_9 (Figure 7). Likewise, an individual bitter neuron may express a large number of *Gr-GAL4* lines, *e.g.* S_6 expresses 28 drivers, whereas others express only a few, *e.g.* the bitter neuron of I_6 expresses only 6 drivers.

We note with special interest that five drivers, *Gr32a*, *Gr33a*, *Gr39a.a*, *Gr66a* and *Gr89a*, are expressed in all bitter neurons. This ubiquitous expression suggests a unique function for these receptors. In support of this suggestion, genetic analysis indicates that Gr33a is broadly required for responses to aversive cues important for both feeding and courtship behaviors (Moon et al., 2009).

We performed a hierarchical cluster analysis of sensilla based on their *Gr-GAL4* expression profiles and identified five classes of sensilla (Figure 8A). These classes, defined by expression analysis, corresponded closely to the five classes defined by functional analysis (Figure 4A). The classifications agreed for 29 of the 31 sensilla.

These results establish a receptor-to-neuron map (Figure 8B). Taken together with the functional map (Figure 4) they provide a receptor-to-neuron-to-response map. The mapping reveals a correlation between the tuning breadth of a bitter-sensitive neuron and the number of *Gr-GAL4* drivers it expresses. The broadly tuned S-a and S-b neurons express 29 and 16 *Gr-GAL4* drivers, respectively, while the more narrowly tuned I-a and I-b neurons express 6 and 10 *Gr-GAL4* drivers, respectively.

In summary, we have generated a receptor-to-neuron map of an entire family of chemosensory receptors and an entire ensemble of taste neurons in a major taste organ. Our data support a role for 33 *Gr* genes in the perception of bitter taste.

Misexpression of a Gr confers physiological responses

The receptor-to-neuron map makes predictions about the functions of certain receptors. For example, according to the map only one receptor, Gr59c, is expressed by I-a but not I-b sensilla. I-a sensilla respond most strongly to berberine, denatonium and lobeline, whereas I-b sensilla show little or no response to these compounds. These results suggested the possibility that Gr59c might act in the response to these compounds.

To test this possibility, we expressed *UAS-Gr59c* in I-b sensilla using *Gr66a-GAL4*. We found that expression of Gr59c in fact conferred strong responses to berberine, denatonium and lobeline when expressed in each of three I-b sensilla, I_{10}, I_9, and I_8 (Figure 9).

We also tested the effects of driving Gr59c expression in sensilla of the I-a, S-a and S-b classes, which show moderate or strong responses to these compounds in wild type. I-a and S-a sensilla express Gr59c in wild type, but we reasoned that the use of the GAL4 system would increase the levels of its expression. We found that misexpression of Gr59c increased the responses to these compounds in all of these sensilla (Figure 9).

We also tested responses to azadirachtin and caffeine, which were not predicted by the receptor-to-neuron map to act via Gr59c. We found that expression of Gr59c did not increase the response to either tastant (Figure S4). Unexpectedly, responses were decreased by ectopic expression of Gr59c in many cases. One possible interpretation of these results is that misexpressed Gr59c titrates out other receptors or cofactors, thereby perturbing the formation of a receptor complex required for the endogenous response. This view is supported by observations that *Gr* gene dosage scales with physiological and/or behavioral responses (Kwon et al., 2007; Tanimura et al., 1988), and by genetic analysis indicating a role for a heteromeric complex of more than three Gr proteins in the detection of caffeine (Lee et al., 2009; Moon et al., 2006; Moon et al., 2009).

We next drove *Gr59c* in sugar neurons, either singly or in combination with *Gr66a* or *Gr33a*, using the *Gr5a-GAL4* driver. Misexpression of *Gr59c* did not confer physiological responses to berberine or other tested bitter compounds in sugar neurons (data not shown). These results suggest that Gr59c is not sufficient for the response to these compounds and likely acts in concert with other Gr proteins and/or cofactors that are specific to bitter neurons.

According to the receptor-to-neuron map, Gr59c is expressed in I-a sensilla along with five other Grs that are broadly expressed in all classes of bitter neurons. Taken together, our results support the hypothesis that Gr59c operates together with one or more of these other Grs, and our analysis confirms the prediction that Gr59c acts in response to at least three bitter tastants.

Discussion

We have provided a systematic behavioral, cellular, and molecular analysis of bitter taste in *Drosophila*. The analysis has revealed extensive complexity in the coding of bitter taste.

Functional diversity of bitter neurons

We have defined five distinct classes of sensilla in the *Drosophila* labellum on the basis of their responses to bitter compounds. Four of these sensillar classes contain bitter-sensing neurons; other sensilla did not respond physiologically to any of our bitter tastants. This analysis, then, has defined four classes of bitter-sensing neurons that are diverse in their response profiles. Some are broadly tuned with respect to a panel of bitter compounds and some are more narrowly tuned. The neurons also vary in the temporal dynamics of their responses. Different neurons respond to the same tastant with different onset kinetics, and an individual neuron responds to distinct tastants with diverse dynamics. The functional diversity of bitter-sensing neurons expands the coding capacity of the system: different tastants elicit responses from different subsets of neurons, and distinct tastants elicit diverse temporal patterns of activity from these neurons.

Our systematic analysis does not support previous models that suggest functional uniformity among bitter neurons (Cobb et al., 2009; Marella et al., 2006). A previous physiological study of the labellum did not reveal functionally distinct neuronal classes, but was limited in the number of sensilla and tastants that were examined (Hiroi et al., 2004). There are major technical challenges in recording from I and S sensilla; the S sensilla in particular are small, curved, and difficult to access because of their position on the labellar surface. Our finding of functional heterogeneity in labellar sensilla is consistent with the finding that two taste sensilla on the prothoracic leg responded to berberine but not quinine, whereas another sensillum responded to quinine but not berberine (Meunier et al., 2003). A recent study found that DEET elicited different responses from several labellar sensilla tested (Lee et al., 2010). Functionally distinct bitter neurons have also been described in taste organs of

caterpillars, and in the case of the *Manduca* larva, aristolochic acid and salicin activate spike trains that differ in dynamics (Glendinning et al., 2006; Glendinning et al., 2002).

Molecular diversity of bitter neurons

The functional differences among neurons in the *Drosophila* labellum suggested underlying molecular differences. In particular, we wondered whether the four classes of bitter taste neurons defined by physiological analysis could be distinguished by molecular analysis. We constructed a receptor-to-neuron map of the entire Gr repertoire and found that four classes of bitter taste neurons emerged on the basis of receptor expression, classes that coincided closely with the four functional classes. Moreover, the neuronal classes that were more broadly tuned expressed more receptors.

While the physiological and molecular analyses support each other well, there are limitations to each analysis that raise interesting considerations. Our functional analysis is based on a limited number of taste stimuli. We selected bitter tastants that were structurally diverse, but bitter compounds vary enormously in structure and only a small fraction of them can be sampled. It is possible that by testing more tastants, by testing them over a greater concentration range, or by analyzing temporal dynamics in greater detail, that even more diversity would become apparent among the bitter-sensing neurons.

There are also limitations to our receptor-to-neuron map. First, the map considers exclusively the 68 Grs. There are at least two additional receptors that can mediate bitter taste. DmXR, a G-protein coupled receptor, is expressed in bitter neurons of the labellum and is required for behavioral avoidance of L-canavanine, a naturally occurring insecticide (Mitri et al., 2009); the TRPA1 cation channel, also expressed in a subset of bitter neurons in the labellum, is required for behavioral and electrophysiological responses to aristolochic acid (Kim et al., 2010). Second, *Gr-GAL4* drivers may not provide a fully accurate representation of *Gr* gene expression in every case. Genetic analysis has shown that *Gr64a* is required for the physiological responses of labellar sensilla to some sugars and is therefore expected to be expressed in labellar sugar neurons (Dahanukar et al., 2007). Our *Gr64a-GAL4* driver, however, is not expressed in these neurons, suggesting the lack of a regulatory element. In light of the limitations to the use of the *GAL4* system to assess receptor expression, we were encouraged that drivers representing all 68 Grs were expressed in chemosensory neurons, with very few exceptions (Figure 6, Table S3 and data not shown), and that the expression patterns in the labellum agreed well with the patterns of physiological responses (Figures 4 and 8). In addition, we were able to integrate the functional and expression data and predict a function for one Gr (Figure 9).

While our data support the hypothesis that *Gr59c* encodes a bitter receptor for berberine, denatonium and lobeline, Gr59c is not sufficient for responses to these compounds in sugar neurons. It is also apparently not necessary, in the sense that physiological responses to these tastants were observed in S-a sensilla that do not express the *Gr59c* driver. These observations suggest that there is another receptor for berberine, denatonium and lobeline that may recognize a different moiety of these tastants, providing multiple means of detecting some of the most behaviorally aversive bitter tastants in the panel.

We note that 38 of the *Gr-GAL4* drivers, slightly more than half, showed expression in the labellum. The other Grs are likely expressed in other chemosensory neurons of the adult and larva (Dunipace et al., 2001; Jones et al., 2007; Kwon et al., 2007; Scott et al., 2001; Thorne and Amrein, 2008) (A.D., J.Y.K., L.W., F. Ling, and J.C., unpublished results). Of the 38 labellar *Gr-GAL4* drivers, 33 are expressed in bitter neurons, and only a few in sugar neurons. It seems likely that a high fraction of Grs are devoted to bitter perception because of the number and structural complexity of bitter compounds (Schoonhoven et al., 2005;

Schwab, 2003). Sugars are simpler and more similar in structure. In order to detect the wide diversity of noxious bitter substances that an animal may encounter, a larger and more versatile repertoire of receptors is likely needed. We note that in mice and rats, 36 bitter receptors have been identified (Wu et al., 2005), but few sugar receptors (Montmayeur et al., 2001; Nelson et al., 2001).

Among the Grs mapped to bitter neurons, five map to all bitter neurons: Gr32a, Gr33a, Gr39a.a, Gr66a, and Gr89a. Some or all of these "core bitter Grs" may function as coreceptors, perhaps forming multimers with other Grs. These core Grs might play a role analogous to Or83b, an Or that is broadly expressed in olfactory receptor neurons and that functions in the transport of other Ors and as a channel, rather than conferring odor-specificity *per se* (Benton et al., 2006; Sato et al., 2008; Wicher et al., 2008). If so, the core Grs may be useful in deorphanizing other Grs in heterologous expression systems. We note that in mammals, T1R3 functions as a common coreceptor with either T1R1 or T1R2 to mediate gustatory responses to amino acids or sugars, respectively (Zhao et al., 2003).

We note finally that the receptor-to-neuron map defines intriguing developmental problems. How do the five classes of sensilla acquire their diverse functional identities? How does an individual taste neuron select, from among a large *Gr* repertoire, which receptor genes to express? In the olfactory system of the fly, the expression of each receptor gene is dictated by a combinatorial code of cis-regulatory elements and by a combinatorial code of transcription factors (Bai and Carlson, 2010; Bai et al., 2009; Clyne et al., 1999; Miller and Carlson, 2010; Ray et al., 2007; Ray et al., 2008; Tichy et al., 2008). Mechanisms of receptor gene choice were elucidated in part by identifying upstream regulatory elements that were common to coexpressed *Or* genes. The receptor-to-neuron map that we have established for the taste system lays a foundation for identifying regulatory elements shared by coexpressed *Gr* genes, which in turn may elucidate mechanisms of receptor gene choice in the taste system. It will be interesting to determine whether the mechanisms used in the olfactory and taste systems are similar.

Taste coding in the labellum

In principle the design of the *Drosophila* taste system could have been extremely simple. Every sensillum could be identical, and all sensilla could report uniformly the valence of each tastant, *e.g.* positive for most sugars and negative for bitter compounds. Such a design would be economical to encode in the genome and to execute during development.

The design of the *Drosophila* olfactory system is not so simple. Physiological analysis of the fly has identified ≥17 functionally distinct types of olfactory sensilla (Clyne et al., 1997; de Bruyne et al., 1999; de Bruyne et al., 2001; Elmore et al., 2003; van der Goes van Naters and Carlson, 2007; Yao et al., 2005). This design allows for the combinatorial coding of odors. A recent study of the *Drosophila* larva defined an odor space in which each dimension represents the response of each component of olfactory input (Kreher et al., 2008). The distance between two odors in this space was proportional to the perceptual relationship between them. In principle, a coding space of high dimension may enhance sensory discrimination and allow for a more adaptive behavioral response to a sensory stimulus.

Here we have found that the fly's taste system is similar to its olfactory system in that its sensilla fall into at least five functionally distinct types, four of which respond to bitter stimuli. This heterogeneity provides the basis for a combinatorial code for tastes and for a multidimensional taste space. A recent report has suggested that flies can not discriminate between pairs of bitter stimuli when applied to leg sensilla (Masek and Scott, 2010); it will be interesting to extend such analysis to the labellum, and especially to examine pairs of

stimuli that have been shown to activate distinct populations of neurons. Our physiological analysis thus invites an extensive behavioral analysis, beyond the scope of the current study, which explores the extent to which such a taste space supports taste discrimination in the fly.

Why might there be selective pressure to enhance the coding of bitter taste? Why not simply coexpress all bitter receptors in one type of neuron that activates a single circuit, thereby triggering equivalent avoidance of all bitter compounds? Not all bitter compounds are equally toxic, and it is not clear that there is a direct correlation between bitterness and toxicity (Glendinning, 1994). It is even possible that in certain contexts, such as the selection of egg-laying sites or self-medication, some bitter tastants may have a positive valence (Singer et al., 2009; Yang et al., 2008). We note that in our behavioral analysis, flies tended to be more sensitive to bitter compounds that activate I-a than I-b neurons, suggesting that I-a ligands are perceived to be more bitter than those of I-b ligand, as if I-a ligands were more toxic. A more nuanced behavioral decision based on the intensities of bitter compounds may exist within the complex milieu of rotting fruit.

The olfactory and taste systems of the fly differ in the anatomy of their projections to the brain. Olfactory receptor neurons (ORNs) project to the antennal lobe, which consists of spherical modules called glomeruli (Su et al., 2009). ORNs of a particular functional specificity converge upon a common glomerulus, and there is a distinct glomerulus for each type of ORN. Taste neurons project from the labellum to a region of the ventral brain called the subesophageal ganglion (SOG) that does not have such an obviously modular structure (Power, 1943; Stocker, 1994; Stocker and Schorderet, 1981). A study using *Gr66a-GAL4*, which marks all or almost all bitter cells in the labellum, and *Gr5a-GAL4*, which marks all or almost all sugar cells, revealed that the two classes of cells project to spatially segregated regions of the SOG (Thorne et al., 2004; Wang et al., 2004). However, subsets of bitter cells labeled by *Gr-GAL4* drivers did not show obvious spatial segregation within the region of the SOG labeled by *Gr66a-GAL4.* Markers of different subsets of sugar cells also showed overlapping projections in the SOG. These studies did not, then, reveal at a gross level the kind of spatially discrete projections that are characteristic of the olfactory system.

However, analysis of the SOG at higher resolution has recently revealed more detailed substructure (Miyazaki and Ito, 2010). Different sets of *Gr66a*-expressing neurons, such as those expressing *Gr47a*, an I-b-specific receptor, showed distinguishable projection patterns, leading to the suggestion that different subregions process different subsets of bitter compounds. Moreover, similarity in projection patterns does not imply identity of function. For example, in the antennal lobe, ORNs that express the odor receptor Or67d converge on the DA1 glomerulus in both males and females, but the projections from DA1 to the protocerebrum are sexually dimorphic (Datta et al., 2008). Activation of these ORNs elicits different behaviors in males and females (Kurtovic et al., 2007). Taste neurons that project to similar locations in the SOG could also activate different circuits, with distinguishable behavioral consequences. Like the fly taste system, the *C. elegans* olfactory system does not contain glomeruli and its sensory neurons coexpress many receptors, yet the worm is able to discriminate odors (Bargmann, 2006). Finally, we note that different sensory neurons that project to similar positions may carry distinguishable information by virtue of differences in the temporal dynamics of their firing (Wilson and Mainen, 2006). We have in fact identified differences in the temporal dynamics elicited by different tastants (Figure 5). In summary, it is difficult to draw definitive conclusions about the functional roles of taste neurons from the currently available anatomical analysis.

A final consideration raised by our analysis is how the responses of the different functional classes of taste sensilla are temporally integrated to control feeding behavior. The different functional classes of sensilla differ in length and are located in different regions of the

labellar surface. Moreover, during the course of feeding the labellum expands, changing the positions of the various sensilla with respect to the food source. It seems likely that there is a temporal order in which labellar taste sensilla send information to the CNS.

In summary, we have provided a systematic behavioral, physiological, and molecular analysis of the primary representation of bitter compounds in a major taste organ. We have defined the molecular and cellular organization of the bitter-sensitive neurons, and we have found extensive functional diversity in their responses. The results provide a foundation for investigating how this primary tastant representation is transformed into successive representations in the CNS and ultimately into behavior.

Experimental Procedures

Drosophila Stocks

Flies were grown on standard cornmeal/agarose culture medium. *Canton-S* flies that were used for electrophysiological recordings and behavior experiments were raised at room temperature (23°C ± 2°C), while transgenic flies used for both recordings and GFP visualization were raised at 25°C. For electrophysiological recordings, freshly eclosed flies were transferred to fresh food and allowed to age for 5–7 days prior to experimentation. For GFP visualization, most lines (72%) were doubly homozygous for the *Gr-GAL4* driver and for the *UAS-mCD8:GFP* reporter; the remaining lines were homozygous lethal. Flies were aged 5–15 days and maintained at 25°C until dissection. Only males were used for all electrophysiological, expression, and behavioral studies. All transgenic constructs were injected into w^{1118} flies.

Transgenic Flies

w;UAS-mCD8-GFP was used as the GFP reporter and *Gr66a-RFP* was from Dahanukar et al., 2007.

For *Gr-GAL4* constructs, primers were used to amplify DNA sequences upstream of the translation initiation codon of gustatory receptor genes using *Canton-S* genomic DNA as a template. Constructs were cloned into pG4PN (Brand and Perrimon, 1993). The size of the promoters varied (Table S3), but was generally dictated by the distance between the translation initiation codon of the *Gr* gene and the coding region of the next 5' gene. The average promoter size was 3.9 kb. Additional lines were kindly provided by H. Amrein (*Gr28a-GAL4*, *Gr28b.d-GAL4*, *Gr59b-GAL4* and *Gr68a-GAL4*) and K. Scott (*Gr21a-GAL4*, *Gr22c-GAL4*, *Gr28b.e-GAL4* and *Gr47a-GAL4*). Samples were analyzed using a Bio-Rad 1024 laser-scanning confocal microscope.

The coding region of *Gr59c* was amplified from *Canton-S* cDNA prepared from labella and was inserted into the pUAST expression vector (Brand and Perrimon, 1993). Two independent lines were tested physiologically.

Tastants

For electrophysiological recordings, tastants were dissolved in 30 mM tricholine citrate (TCC; Sigma-Aldrich, St. Louis, MO), an electrolyte that inhibits the activity of the water cell (Wieczorek and Wolff, 1989); for the behavioral assay, tastants were dissolved in water. All tastants were stored at −20°C, and aliquots were kept at 4°C and used for no more than one week. Tastants of the highest available purity were obtained from Sigma-Aldrich and stored as recommended. All tastants were tested at the following concentrations unless otherwise indicated: aristolochic acid (ARI), 1 mM; azadirachtin (AZA), 1 mM; berberine chloride (BER), 1 mM; caffeine (CAF), 10 mM; coumarin (COU), 10 mM; N,N-Diethyl-*m*-

toluamide (DEET), 10 mM; denatonium benzoate (DEN), 10 mM; escin (ESC), 10 mM; gossypol from cotton seeds (GOS), 1 mM; (−)-lobeline hydrochloride (LOB), 1 mM; saponin from quillaja bark (SAP), 1%; D-(+)-sucrose octaacetate (SOA), 1 mM; sparteine sulfate salt (SPS), 10 mM; strychnine nitrate salt (STR), 10 mM; theophylline (TPH), 10 mM; and umbelliferone (UMB), 10 mM. Additional tastants that did not elicit physiological responses >10 spikes/s in limited testing included gibberellic acid (10 mM), (−)-catechin (1 mM), cucubertacin I hydrate (1 mM), atropine (1 mM), *N*-phenylthiourea (1 mM), harmaline (1 mM), (−)-nicotine (10 mM), gallic acid (10 mM), (−)-sinigrin hydrate (10 mM), theobromine (10 mM), α-(methylaminomethly)benzyl alcohol (10 mM) and naringen (1 mM).

Electrophysiology

Extracellular single-unit recordings were performed using the tip-recording method (Hodgson et al., 1955). Flies were immobilized via a reference electrode containing *Drosophila* Ringer solution which was threaded through the thorax and head to the tip of the labellum. This electrode served as the indifferent electrode. Tastants were introduced to individual sensilla via a glass recording electrode (10–15 μm tip diameter) filled with tastant solution. Traces of action potentials were recorded using TasteProbe (Syntech, The Netherlands) and analyzed using Autospike 3.2 software (Syntech). Responses were quantified by counting the number of spikes generated over a 500 ms period beginning 200 ms after contact. When measuring latencies in spike generation, only traces in which the first contact was successful were used for our calculations.

In some recordings, sensilla or groups of sensilla were anomalously unresponsive, presumably due to damage resulting from the insertion of the reference electrode. We therefore tested the viability of labellar sensilla with a positive control (for example, berberine was used to test I-a sensilla and caffeine was used to test I-b sensilla). A maximum of 8 tastants were tested on a single sensillum with a minimum of 5 minutes between presentations.

Behavioral Assays

The two-choice assay was performed with minor modifications of the original protocol (Tanimura et al., 1982). Fifty flies (3–5 days old) were transferred to a vial containing moistened Kimwipes and starved at room temperature for 22 hours. Flies were introduced to a 60-well plate containing alternating wells of 1 mM sucrose (containing 0.5 mg/ml sulforhodamine B, Sigma) or 5 mM sucrose plus bitter tastant (containing 0.25 mg/ml indigo carmine, Sigma) and allowed to feed for 2 hours in the dark at 25°C. Flies were anesthetized by freezing the plates at −20°C and the abdomens were scored blind to experimental condition as red, blue, purple or white. In most trials more than 50% of flies participated, *i.e.* were scored as red, blue, or purple, and only trials in which more than 33% of flies participated were included in our analysis. A minimum of 6 independent trials were performed for each tastant and for each concentration. The preference indices were calculated as follows: P.I. = $(N_{blue} + 0.5\ N_{purple})/(N_{red} + N_{purple} + N_{blue})$, where N_{red}, N_{blue} and N_{purple} represent the number of flies with red, blue and purple abdomens. Control experiments showed that the dyes did not affect preference.

Statistical Analyses

Hierarchical cluster analyses using Ward's method were performed using the statistics program PAST (http://folk.uio.no/ohammer/past) (Hammer et al., 2001). All error bars are standard errors of the mean (SEM).

Supplementary Material

Refer to Web version on PubMed Central for supplementary material.

Acknowledgments

This work was supported by NIH-GM063364. We thank Jennifer Perry for helpful discussions and construction of GAL4 lines. We thank Drs. K. Scott, H. Amrein, and H. Keshishian for sharing reagents.

References

Adler E, Hoon MA, Mueller KL, Chandrashekar J, Ryba NJ, Zuker CS. A novel family of mammalian taste receptors. Cell. 2000; 100:693–702. [PubMed: 10761934]

Bai L, Carlson JR. Distinct functions of *acj6* splice forms in odor receptor gene choice. J Neurosci. 2010; 30:5028–5036. [PubMed: 20371823]

Bai L, Goldman AL, Carlson JR. Positive and negative regulation of odor receptor gene choice in *Drosophila* by acj6. J Neurosci. 2009; 29:12940–12947. [PubMed: 19828808]

Bargmann CI. Chemosensation in *C. elegans*. WormBook. 2006:1–29. [PubMed: 18050433]

Benton R, Sachse S, Michnick SW, Vosshall LB. Atypical membrane topology and heteromeric function of *Drosophila* odorant receptors in vivo. PLoS Biol. 2006; 4:e20. [PubMed: 16402857]

Brand AH, Perrimon N. Targeted gene expression as a means of altering cell fates and generating dominant phenotypes. Development. 1993; 118:401–415. [PubMed: 8223268]

Chyb S, Dahanukar A, Wickens A, Carlson JR. *Drosophila Gr5a* encodes a taste receptor tuned to trehalose. Proc Natl Acad Sci U S A. 2003; 100(Suppl 2):14526–14530. [PubMed: 14523229]

Clyne P, Grant A, O'Connell R, Carlson JR. Odorant response of individual sensilla on the *Drosophila* antenna. Invert Neurosci. 1997; 3:127–135. [PubMed: 9783438]

Clyne PJ, Certel SJ, de Bruyne M, Zaslavsky L, Johnson WA, Carlson JR. The odor specificities of a subset of olfactory receptor neurons are governed by Acj6, a POU-domain transcription factor. Neuron. 1999; 22:339–347. [PubMed: 10069339]

Clyne PJ, Warr CG, Carlson JR. Candidate taste receptors in *Drosophila*. Science. 2000; 287:1830–1834. [PubMed: 10710312]

Cobb M, Scott K, Pankratz M. Gustation in *Drosophila melanogaster*. SEB Exp Biol Ser. 2009; 63:1–38. [PubMed: 19174987]

Dahanukar A, Lei YT, Kwon JY, Carlson JR. Two *Gr* genes underlie sugar reception in *Drosophila*. Neuron. 2007; 56:503–516. [PubMed: 17988633]

Datta SR, Vasconcelos ML, Ruta V, Luo S, Wong A, Demir E, Flores J, Balonze K, Dickson BJ, Axel R. The *Drosophila* pheromone cVA activates a sexually dimorphic neural circuit. Nature. 2008; 452:473–477. [PubMed: 18305480]

de Bruyne M, Clyne PJ, Carlson JR. Odor coding in a model olfactory organ: the *Drosophila* maxillary palp. J Neurosci. 1999; 19:4520–4532. [PubMed: 10341252]

de Bruyne M, Foster K, Carlson JR. Odor coding in the *Drosophila* antenna. Neuron. 2001; 30:537–552. [PubMed: 11395013]

Dethier, VG. The Hungry Fly. Harvard University Press; Cambridge: 1976.

Dunipace L, Meister S, McNealy C, Amrein H. Spatially restricted expression of candidate taste receptors in the *Drosophila* gustatory system. Curr Biol. 2001; 11:822–835. [PubMed: 11516643]

Elmore T, Ignell R, Carlson JR, Smith DP. Targeted mutation of a *Drosophila* odor receptor defines receptor requirement in a novel class of sensillum. J Neurosci. 2003; 23:9906–9912. [PubMed: 14586020]

Falk R, Bleiser-Avivi N, Atidia J. Labellar taste organs of *Drosophila melanogaster*. J Morphol. 1976; 150:327–342.

Fujishiro N, Kijima H, Morita H. Impulse frequency and action potential amplitude in labellar chemosensory neurons of *Drosophila melanogaster*. J Insect Physiol. 1984; 30:317–325.

Glendinning JI. Is the bitter rejection response always adaptive? Physiol Behav. 1994; 56:1217–1227. [PubMed: 7878094]

Glendinning JI, Davis A, Rai M. Temporal coding mediates discrimination of “bitter” taste stimuli by an insect. J Neurosci. 2006; 26:8900–8908. [PubMed: 16943545]

Glendinning JI, Davis A, Ramaswamy S. Contribution of different taste cells and signaling pathways to the discrimination of “bitter” taste stimuli by an insect. J Neurosci. 2002; 22:7281–7287. [PubMed: 12177223]

Hammer O, Harper DAT, Ryan PD. PAST: Paleontological Statistics Software Package for Education and Data Analysis. Palaeontologia Electronica. 2001; 4:1–9.

Hansen SR, Janssen C, Beasley VR. Denatonium benzoate as a deterrent to ingestion of toxic substances: toxicity and efficacy. Vet Hum Toxicol. 1993; 35:234–236. [PubMed: 8351798]

Hiroi M, Marion-Poll F, Tanimura T. Differentiated response to sugars among labellar chemosensilla in *Drosophila*. Zoolog Sci. 2002; 19:1009–1018. [PubMed: 12362054]

Hiroi M, Meunier N, Marion-Poll F, Tanimura T. Two antagonistic gustatory receptor neurons responding to sweet-salty and bitter taste in *Drosophila*. J Neurobiol. 2004; 61:333–342. [PubMed: 15389687]

Hodgson ES, Lettvin JY, Roeder KD. Physiology of a primary chemoreceptor unit. Science. 1955; 122:417–418. [PubMed: 13246649]

Jiao Y, Moon SJ, Wang X, Ren Q, Montell C. Gr64f is required in combination with other gustatory receptors for sugar detection in *Drosophila*. Curr Biol. 2008; 18:1797–1801. [PubMed: 19026541]

Jones WD, Cayirlioglu P, Kadow IG, Vosshall LB. Two chemosensory receptors together mediate carbon dioxide detection in *Drosophila*. Nature. 2007; 445:86–90. [PubMed: 17167414]

Keast RS, Bournazel MM, Breslin PA. A psychophysical investigation of binary bitter-compound interactions. Chem Senses. 2003; 28:301–313. [PubMed: 12771017]

Kim SH, Lee Y, Akitake B, Woodward OM, Guggino WB, Montell C. *Drosophila* TRPA1 channel mediates chemical avoidance in gustatory receptor neurons. Proc Natl Acad Sci U S A. 2010; 107:8440–8445. [PubMed: 20404155]

Koganezawa M, Haba D, Matsuo T, Yamamoto D. The shaping of male courtship posture by lateralized gustatory inputs to male-specific interneurons. Curr Biol. 2010; 20:1–8. [PubMed: 20036540]

Koul, O. Insect Antifeedants. CRC Press; Boca Raton: 2005.

Kreher SA, Mathew D, Kim J, Carlson JR. Translation of sensory input into behavioral output via an olfactory system. Neuron. 2008; 59:110–124. [PubMed: 18614033]

Kurtovic A, Widmer A, Dickson BJ. A single class of olfactory neurons mediates behavioural responses to a *Drosophila* sex pheromone. Nature. 2007; 446:542–546. [PubMed: 17392786]

Kwon JY, Dahanukar A, Weiss LA, Carlson JR. The molecular basis of CO_2 reception in *Drosophila*. Proc Natl Acad Sci U S A. 2007; 104:3574–3578. [PubMed: 17360684]

Lee Y, Kim SH, Montell C. Avoiding DEET through insect gustatory receptors. Neuron. 2010; 67:555–561. [PubMed: 20797533]

Lee Y, Moon SJ, Montell C. Multiple gustatory receptors required for the caffeine response in *Drosophila*. Proc Natl Acad Sci U S A. 2009; 106:4495–4500. [PubMed: 19246397]

Marella S, Fischler W, Kong P, Asgarian S, Rueckert E, Scott K. Imaging taste responses in the fly brain reveals a functional map of taste category and behavior. Neuron. 2006; 49:285–295. [PubMed: 16423701]

Masek P, Scott K. Limited taste discrimination in *Drosophila*. Proc Natl Acad Sci U S A. 2010; 107:14833–14838. [PubMed: 20679196]

Meunier N, Marion-Poll F, Rospars JP, Tanimura T. Peripheral coding of bitter taste in *Drosophila*. J Neurobiol. 2003; 56:139–152. [PubMed: 12838579]

Miller CJ, Carlson JR. Regulation of odor receptor genes in trichoid sensilla of the *Drosophila* antenna. Genetics. 2010; 186:79–95. [PubMed: 20551440]

Mitri C, Soustelle L, Framery B, Bockaert J, Parmentier ML, Grau Y. Plant insecticide L-canavanine repels *Drosophila* via the insect orphan GPCR DmX. PLoS Biol. 2009; 7:e1000147. [PubMed: 19564899]

Miyazaki T, Ito K. Neural architecture of the primary gustatory center of *Drosophila melanogaster* visualized with GAL4 and LexA enhancer-trap systems. J Comp Neurol. 2010; 518:4147–4181. [PubMed: 20878781]

Montmayeur JP, Liberles SD, Matsunami H, Buck LB. A candidate taste receptor gene near a sweet taste locus. Nat Neurosci. 2001; 4:492–498. [PubMed: 11319557]

Moon SJ, Kottgen M, Jiao Y, Xu H, Montell C. A taste receptor required for the caffeine response *in vivo*. Curr Biol. 2006; 16:1812–1817. [PubMed: 16979558]

Moon SJ, Lee Y, Jiao Y, Montell C. A *Drosophila* gustatory receptor essential for aversive taste and inhibiting male-to-male courtship. Curr Biol. 2009; 19:1623–1627. [PubMed: 19765987]

Mueller KL, Hoon MA, Erlenbach I, Chandrashekar J, Zuker CS, Ryba NJ. The receptors and coding logic for bitter taste. Nature. 2005; 434:225–229. [PubMed: 15759003]

Nathans J. The genes for color vision. Sci Am. 1989; 260:42–49. [PubMed: 2643825]

Nayak SV, Singh RN. Sensilla on the tarsal segments and mouthparts of adult *Drosophila melanogaster* meigen (Diptera : Drosophilidae). International Journal of Insect Morphology and Embryology. 1983; 12:273–291.

Nelson G, Hoon MA, Chandrashekar J, Zhang Y, Ryba NJ, Zuker CS. Mammalian sweet taste receptors. Cell. 2001; 106:381–390. [PubMed: 11509186]

Power ME. The brain of *D. melanogaster*. J Morphol. 1943; 72:517–559.

Ray A, van Naters WG, Shiraiwa T, Carlson JR. Mechanisms of odor receptor gene choice in *Drosophila*. Neuron. 2007; 53:353–369. [PubMed: 17270733]

Ray A, van Naters WV, Carlson JR. A regulatory code for neuron-specific odor receptor expression. Plos Biology. 2008; 6:1069–1083.

Robertson HM, Warr CG, Carlson JR. Molecular evolution of the insect chemoreceptor gene superfamily in *Drosophila melanogaster*. Proc Natl Acad Sci U S A. 2003; 100(Suppl 2):14537–14542. [PubMed: 14608037]

Rodrigues V, Siddiqi O. Genetic-Analysis of Chemosensory Pathway. Proc Indian Acad Sci [B]. 1978; 87:147–160.

Sato K, Pellegrino M, Nakagawa T, Nakagawa T, Vosshall LB, Touhara K. Insect olfactory receptors are heteromeric ligand-gated ion channels. Nature. 2008; 452:1002–1006. [PubMed: 18408712]

Schoonhoven, LM.; Van Loon, JJA.; Dicke, M. Insect-plant biology. Oxford University Press; Oxford: 2005.

Schwab W. Metabolome diversity: too few genes, too many metabolites? Phytochemistry. 2003; 62:837–849. [PubMed: 12590111]

Scott K, Brady R Jr. Cravchik A, Morozov P, Rzhetsky A, Zuker C, Axel R. A chemosensory gene family encoding candidate gustatory and olfactory receptors in *Drosophila*. Cell. 2001; 104:661–673. [PubMed: 11257221]

Shanbhag SR, Park SK, Pikielny CW, Steinbrecht RA. Gustatory organs of *Drosophila melanogaster*: fine structure and expression of the putative odorant-binding protein PBPRP2. Cell Tissue Res. 2001; 304:423–437. [PubMed: 11456419]

Singer MS, Mace KC, Bernays EA. Self-medication as adaptive plasticity: increased ingestion of plant toxins by parasitized caterpillars. PLoS ONE. 2009; 4:e4796. [PubMed: 19274098]

Slone J, Daniels J, Amrein H. Sugar receptors in *Drosophila*. Curr Biol. 2007; 17:1809–1816. [PubMed: 17919910]

Stocker RF. The organization of the chemosensory system in *Drosophila melanogaster*: a review. Cell Tissue Res. 1994; 275:3–26. [PubMed: 8118845]

Stocker RF, Schorderet M. Cobalt filling of sensory projections from internal and external mouthparts in *Drosophila*. Cell Tissue Res. 1981; 216:513–523. [PubMed: 6786751]

Su CY, Menuz K, Carlson JR. Olfactory perception: receptors, cells, and circuits. Cell. 2009; 139:45–59. [PubMed: 19804753]

Tanimura T, Isono K, Takamura T, Shimada I. Genetic dimorphism in the taste sensitivity to trehalose in *Drosophila melanogaster*. Journal of Comparative Physiology. 1982; 147:433–437.

Tanimura T, Isono K, Yamamoto M. Taste sensitivity to trehalose and its alteration by gene dosage in *Drosophila melanogaster*. Genetics. 1988; 119:399–406. [PubMed: 17246428]

Thorne N, Amrein H. Atypical expression of *Drosophila* gustatory receptor genes in sensory and central neurons. J Comp Neurol. 2008; 506:548–568. [PubMed: 18067151]

Thorne N, Chromey C, Bray S, Amrein H. Taste perception and coding in *Drosophila*. Curr Biol. 2004; 14:1065–1079. [PubMed: 15202999]

Tichy AL, Ray A, Carlson JR. A new *Drosophila* POU gene, *pdm3*, acts in odor receptor expression and axon targeting of olfactory neurons. Journal of Neuroscience. 2008; 28:7121–7129. [PubMed: 18614681]

van der Goes van Naters W, Carlson JR. Receptors and neurons for fly odors in *Drosophila*. Curr Biol. 2007; 17:606–612. [PubMed: 17363256]

Wang Z, Singhvi A, Kong P, Scott K. Taste representations in the *Drosophila* brain. Cell. 2004; 117:981–991. [PubMed: 15210117]

Wicher D, Schafer R, Bauernfeind R, Stensmyr MC, Heller R, Heinemann SH, Hansson BS. *Drosophila* odorant receptors are both ligand-gated and cyclic-nucleotide-activated cation channels. Nature. 2008; 452:1007–1011. [PubMed: 18408711]

Wieczorek H, Wolff G. The labellar sugar receptor of *Drosophila*. J Comp Physiol [A]. 1989; 164:825–834.

Wilson RI, Mainen ZF. Early events in olfactory processing. Annu Rev Neurosci. 2006; 29:163–201. [PubMed: 16776583]

Wu SV, Chen MC, Rozengurt E. Genomic organization, expression, and function of bitter taste receptors (T2R) in mouse and rat. Physiol Genomics. 2005; 22:139–149. [PubMed: 15886333]

Yang CH, Belawat P, Hafen E, Jan LY, Jan YN. *Drosophila* egg-laying site selection as a system to study simple decision-making processes. Science. 2008; 319:1679–1683. [PubMed: 18356529]

Yao CA, Ignell R, Carlson JR. Chemosensory coding by neurons in the coeloconic sensilla of the *Drosophila* antenna. J Neurosci. 2005; 25:8359–8367. [PubMed: 16162917]

Yarmolinsky DA, Zuker CS, Ryba NJ. Common sense about taste: from mammals to insects. Cell. 2009; 139:234–244. [PubMed: 19837029]

Zhao GQ, Zhang Y, Hoon MA, Chandrashekar J, Erlenbach I, Ryba NJ, Zuker CS. The receptors for mammalian sweet and umami taste. Cell. 2003; 115:255–266. [PubMed: 14636554]

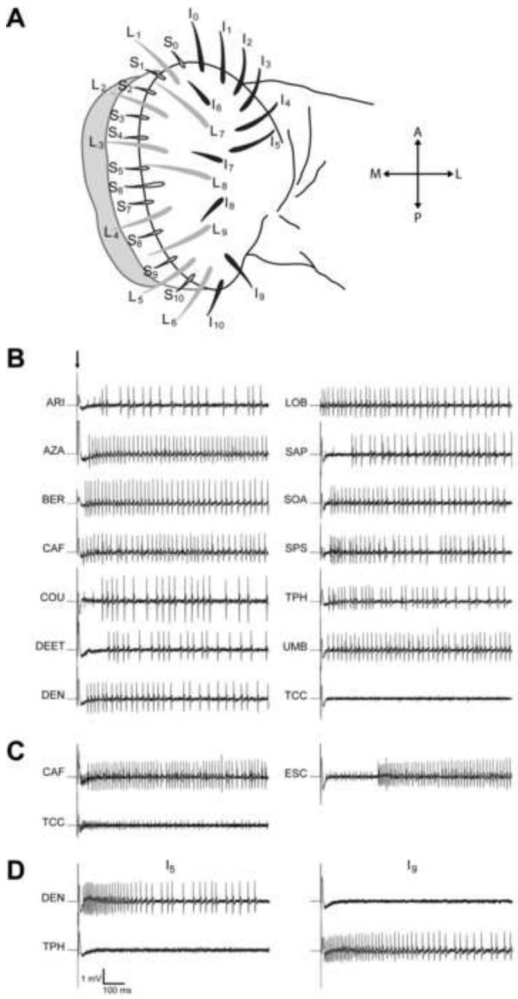

Figure 1.

The *Drosophila* labellum and its physiological responses. (A) A typical *Drosophila* labellum is comprised of two labellar palps, each of which has 31 sensilla that are categorized and numbered based on their position and morphology. We observe some variation in the number of sensilla; *e.g.* either S_0 or S_1 is missing in 54% of labella (n = 78), and the number of anterolateral I sensilla (I_0–I_5) ranges between $5 \leq n \leq 8$ (n = 67). Sensilla are shaded according to their morphological classes. “A” is anterior, “P” is posterior, “M” is medial and “L” is lateral. The numbering and classification of individual sensilla differ slightly from the previous literature (Hiroi et al., 2002; Shanbhag et al., 2001) in order to reflect observations in our laboratory strain. (B and C) Sample traces of physiological recordings from the S_6 (B) and S_9 (C) sensilla. Control traces using the diluent, tricholine citrate (TCC), are shown for both sensilla. (D) Sample traces of physiological recordings from I_5 (left) and I_9 (right) sensilla presented with DEN or TPH demonstrate functional heterogeneity among sensilla. The arrow indicates the contact artifact observed at the beginning of each trace. See Experimental Procedures for tastant abbreviations.

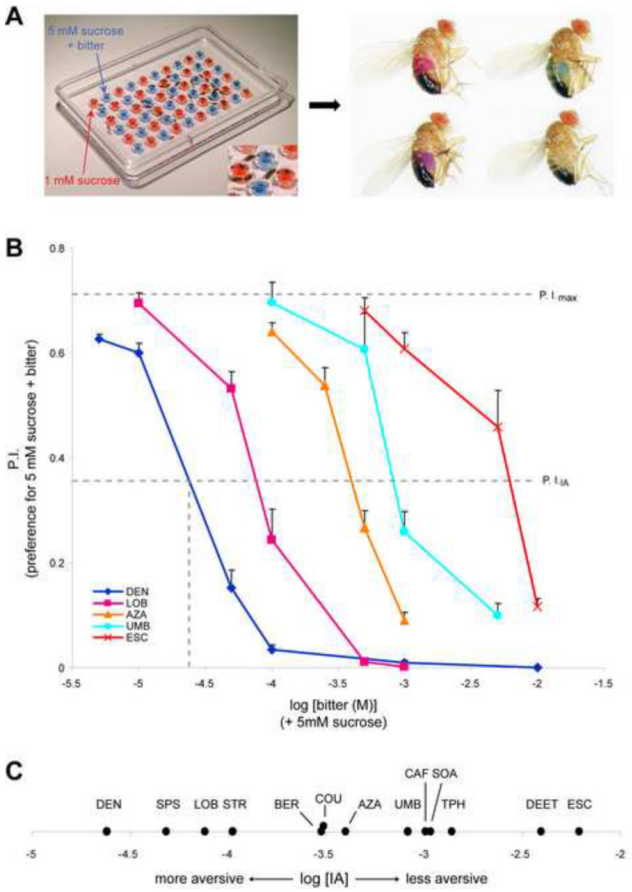

Figure 2.

Drosophila avoid ingesting bitter tastants in a two-choice assay. (A) Flies are allowed to feed on microtiter plates containing alternating wells of either 1 mM sucrose, labeled with a red dye, or a solution of 5 mM sucrose mixed with a bitter tastant, labeled with a blue dye (left). The abdomens are scored as red, blue, purple or uncolored, indicating that the fly ingested the red solution, the blue solution, both solutions, or neither solution (right). (B) The preference indices (P.I.) are plotted for five representative bitter compounds over a range of concentrations; results for other bitter compounds are shown in Figure S1. Error bars are SEM. The dotted line labeled "$P.I._{max}$" indicates the preference for 1 mM sucrose when no bitter is present in the 5 mM sucrose solution (P.I. = 0.71); "$P.I._{IA}$" indicates the P.I. for which the two solutions are isoattractive ($P.I._{IA}$ = 0.36). The vertical dotted line indicates the isoattractive concentration for denatonium. (C) Isoattractive concentrations for each bitter tastant. The isoattractive concentration for SAP is 0.37% but is not plotted in terms of molarity because it has a range of molecular weights (Figure S1B). For each data point, $6 \leq n \leq 7$ trials. The mean percentage of flies that had colored abdomens, averaged over all concentrations of all compounds tested (n = 68), was 65.8%, ranging from 33.9% to 87.0%. (See also Figure S1.)

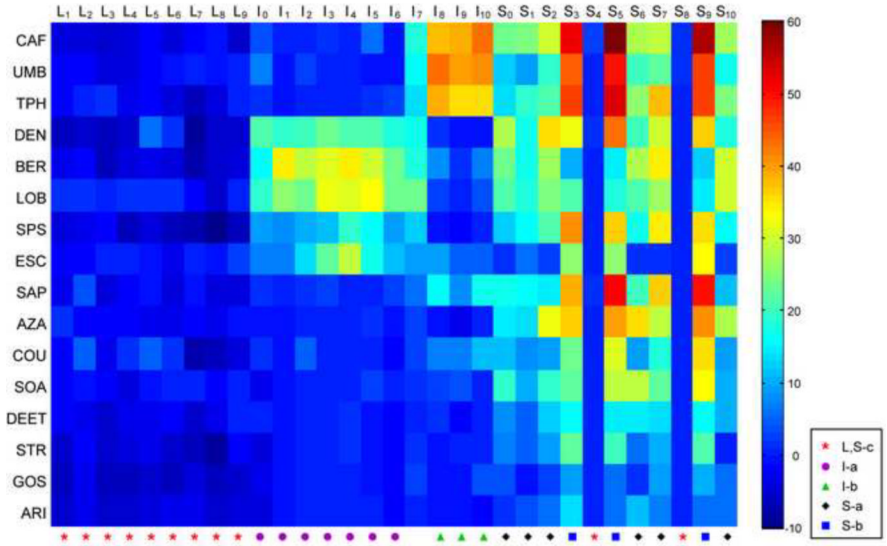

Figure 3.

Labellar sensilla exhibit distinct response profiles to a panel of bitter tastants. The heat map shows the electrophysiological responses of labellar sensilla to a panel of 16 bitter tastants. Responses to the diluent control, 30 mM TCC, were subtracted from each value. Each sensillum's functional class, as described in Figure 4, is identified by a colored symbol for ease of comparison. For each data point, n ≥ 10. (See also Tables S1 and S2 for numerical values.)

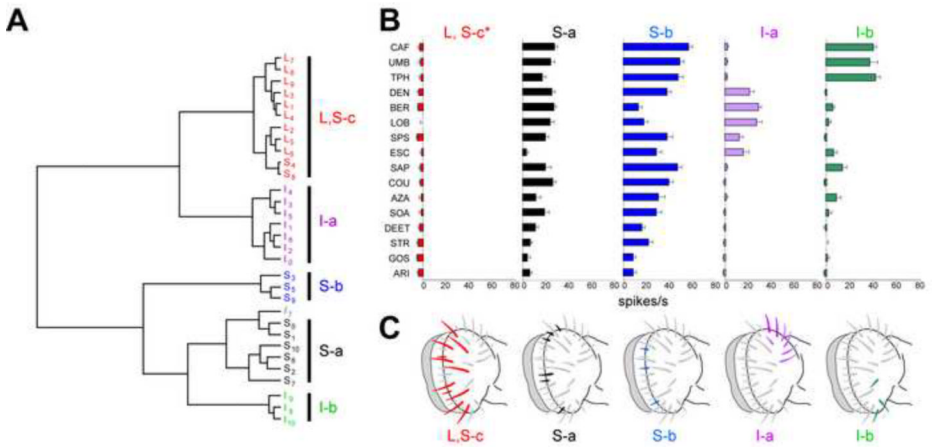

Figure 4.

Labellar sensilla can be clustered into five functional classes on the basis of response spectra. (A) Cluster analysis, based on Ward's method. The diluent control was subtracted from each response. The identity of I_7 was variable and it has therefore not been assigned to any functional class. (B) Mean responses of all sensilla of a given functional class. Responses to the diluent control, TCC, were subtracted. Error bars are SEM. * “L, S-c” sensilla did not exhibit any observable physiological responses to any tested bitter compounds and no “bitter” neuron spikes were identified. The asterisk indicates that spikes from these sensilla were counted somewhat differently; we elected to count all spikes for these sensilla, which show high responses to the control diluent, TCC (Table S1). The activity of the water neuron decreases as osmolarity increases. Thus, the presence of a bitter tastant likely inhibits any remaining water neuron firing, resulting in the observed “negative” values. (C) Distribution of sensilla of each class.

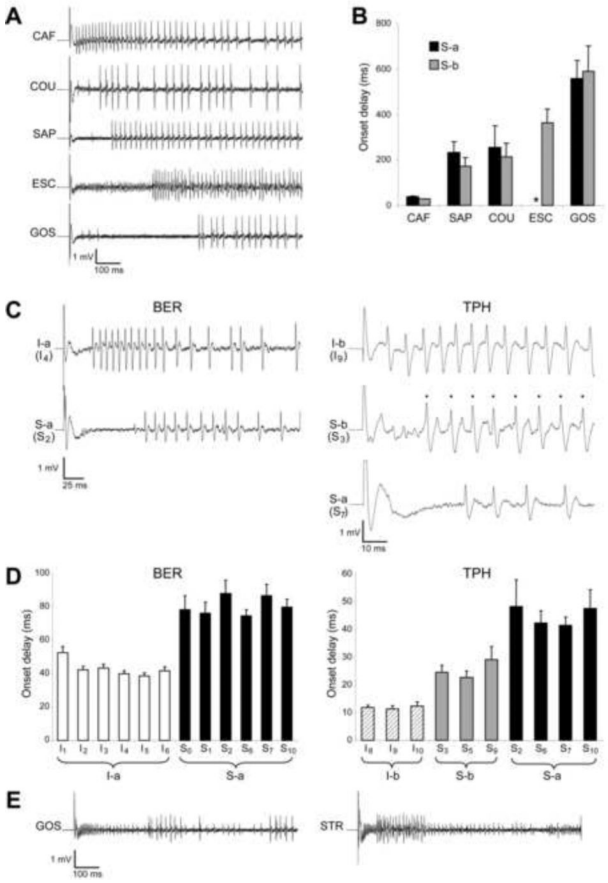

Figure 5.

Sensillar classes exhibit characteristic latencies in spike generation. (A) Sample traces illustrating typical delays in spike onset. Recordings are from the S_6 sensillum stimulated with CAF, COU, SAP or GOS, and the S_9 sensillum stimulated with ESC. (B) The mean delay in spike onset is shown for S-a (represented by S_2, S_6 and S_7) and S-b (represented by S_3, S_5 and S_9) sensilla in response to the indicated tastants. For individual sensilla (not including CAF), $6 \leq n \leq 16$, with a mean of 9.8 traces analyzed. * = no response. (C) Sample traces of recordings from sensilla of the indicated functional classes stimulated with BER (left) or TPH (right). The time scales are expanded in order to illustrate clearly the delays in the onset of spike initiation. The spikes elicited from S_3 by TPH have been marked with dots for clarity. (D) The mean delay in spike onset is shown for sensilla of the indicated functional classes in response to BER (left) or TPH (right). Bars are color-coded by sensillum class. $11 \leq n \leq 40$, with a mean of 21 traces analyzed for each sensillum type. (E) Bursting responses of S_9 sensilla to the indicated tastants. Error bars are SEM. (See also Figure S2.)

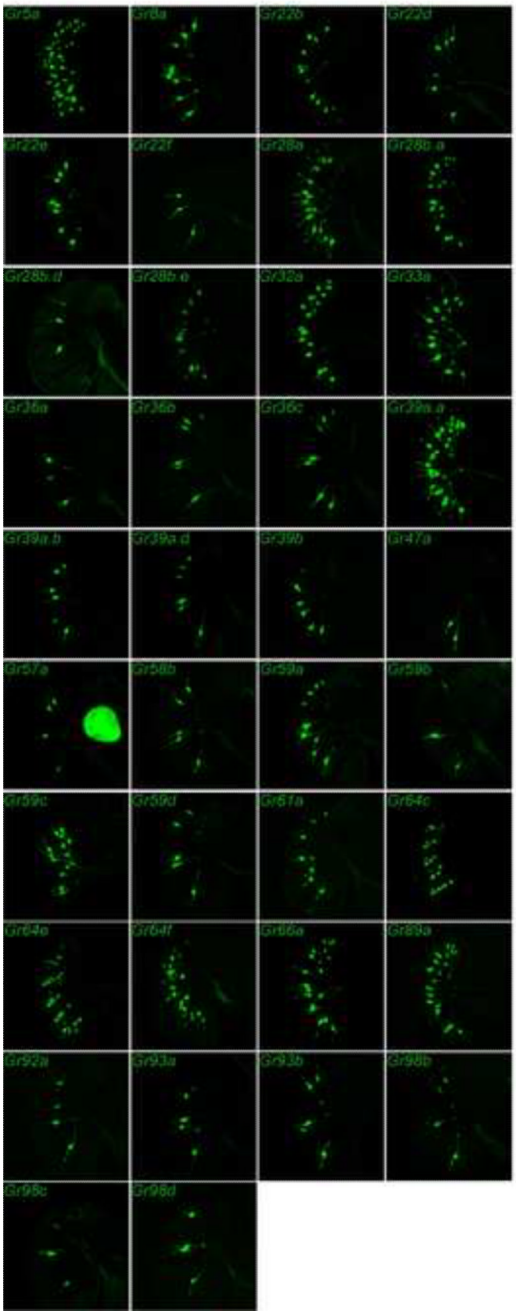

Figure 6.

Expression of *Gr-GAL4* drivers in gustatory sensory neurons of the labellum. Compressed z-stacks of single labellar palps, showing GFP reporter expression. All expression is neuronal, with the exception of a large area in the *Gr57a-GAL4* labellum, tentatively identified as a salivary gland. (See also Figure S3.)

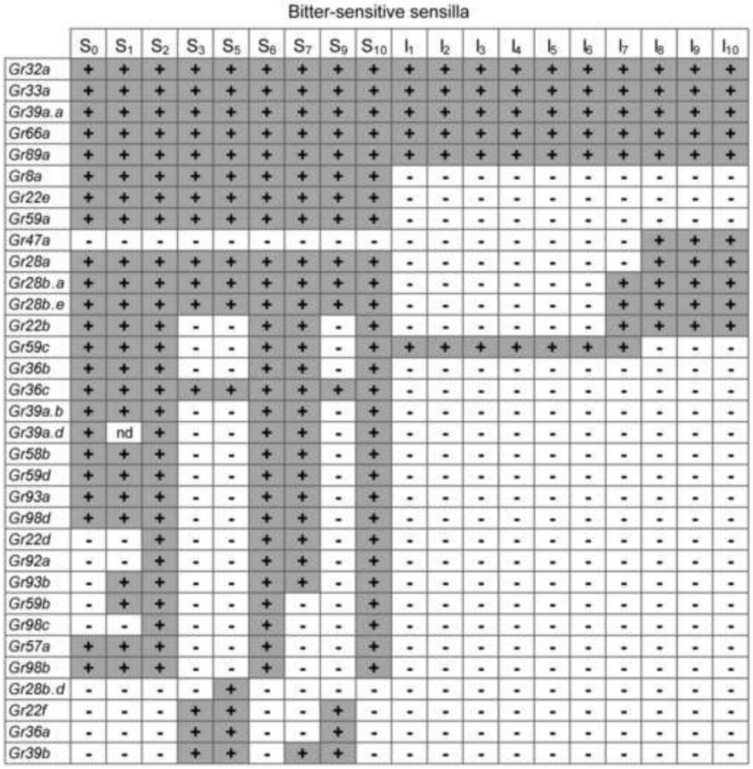

Figure 7.

Individual bitter-sensitive sensilla express distinct subsets of *Gr-GAL4* drivers. *Gr-GAL4* drivers that are expressed in bitter neurons were mapped to individual sensilla. “+” indicates a mean expression value of 0.5 or greater (see Table S3); “−” indicates a value less than 0.5. “nd”, no data.

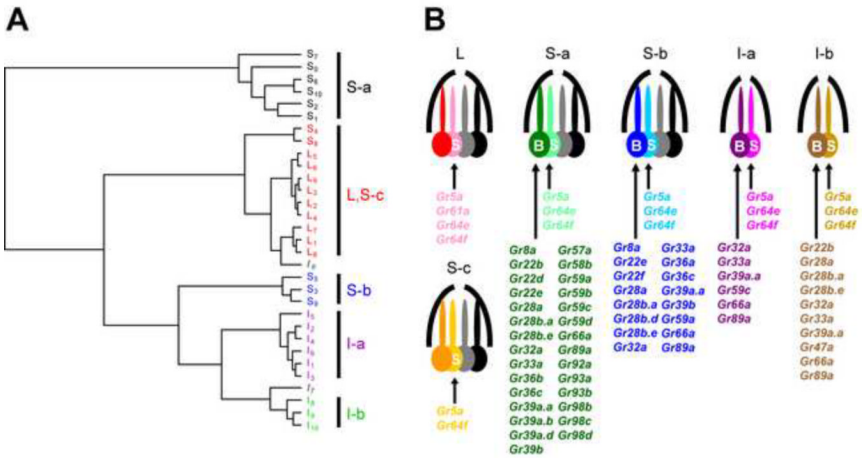

Figure 8.

Labellar sensilla fall into five expression classes that are similar to the functional classes. (A) A hierarchical cluster analysis of sensilla based on their *Gr* gene expression profiles. Ward's method, using numerical data from Table S3, identifies five classes of sensilla. (A similar analysis using only data from *Gr66a*-expressing neurons generates identical classes.) These classes correspond well to the functionally identified classes (Figure 4) and are therefore labeled accordingly. (B) A receptor-to-neuron map is presented for the bitter ("B") and sugar ("S") neurons in all classes of labellar sensilla. (Note that "S" in this case refers to a neuron type and not a sensillum.) The "L" and "S-c" sensilla are grouped together since they generally do not express the "bitter" *Gr-GAL4* drivers, but are indicated separately to reflect differences in the expression profiles of their sugar neurons. We observed expression of *Gr28a-GAL4* and *Gr39a.a-GAL4* in L sensilla but have not mapped them to neurons; there is evidence that the *Gr28a-GAL4* driver is expressed in S neurons of L sensilla (Thorne and Amrein, 2008). I_0 and I_7 do not fit easily into any sensillum class and are therefore not included.

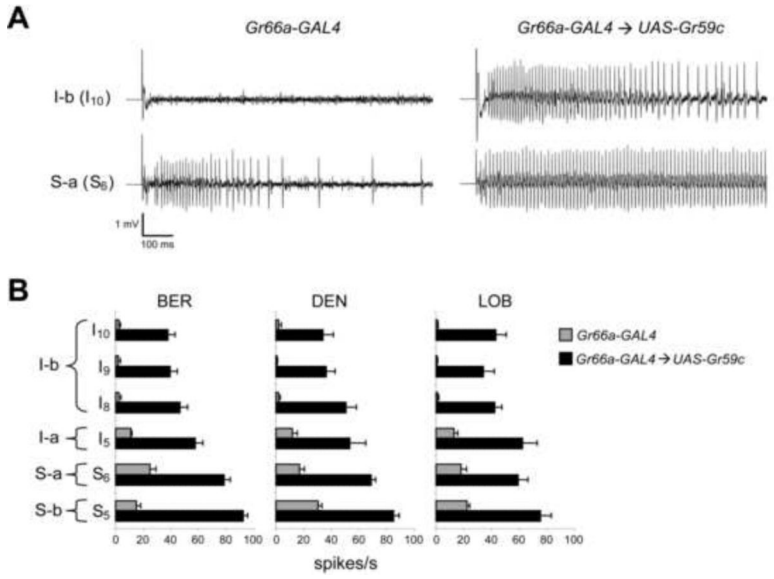

Figure 9.

Misexpression of a receptor confers physiological responses. (A) Sample traces of recordings from I-b and S-a sensilla of the indicated genotypes stimulated with BER. (B) Mean responses of six sensilla representing all four bitter-responsive classes of labellar sensilla to BER, DEN or LOB. $8 \leq n \leq 22$, with a mean of 12 recordings. Similar results were observed for all sensilla of a given class (data not shown). Error bars are SEM. The following genotypes were used: *Sp/CyO; Gr66a-GAL4/TM3* or *UAS-Gr59c/CyO; Gr66a-GAL4/TM3*. (See also Figure S4.)